

Microstructure of plasma-sprayed $\text{YBa}_2\text{Cu}_3\text{O}_x$ high-temperature superconductors

L. PAWLOWSKI, A. GROSS, R. McPHERSON

Department of Materials Engineering, Monash University, Clayton, Victoria 3168, Australia

The arc plasma spraying process has been applied to deposit YBaCuO superconductors on to steel substrates. Detached, as-sprayed coatings were heat treated at 950°C in air in order to restore superconductivity. Oxygen annealing at temperatures $400\text{--}500^\circ\text{C}$ has been used as the final stage in material preparation. The changes in the microstructure of the material during heat treatment have been followed with the aid of scanning electron and optical microscopy. The phase transformations resulting from heat treatment have been studied by differential thermal analysis and X-ray diffraction.

1. Introduction

Since the discovery of superconductivity at 90 K in a $\text{YBa}_2\text{Cu}_3\text{O}_x$ compound by Wu *et al.* [1], a considerable effort has been undertaken in order to determine technologies for material processing. Among many other techniques, thermal spraying has been chosen to deposit superconducting coatings.

Previously published papers have dealt with the following thermal spray techniques: open-air plasma spraying [2–10], vacuum plasma spraying [11], combustion flame spraying [7, 8, 12, 13], hypervelocity flame spraying (so-called JETKOTE process) [2, 14]. Coatings are not superconducting when sprayed on to a cold substrate and they must be heat treated to develop the superconducting orthorhombic phase. A variety of phases has been reported in the as-sprayed deposits [2, 6, 12] but it now appears that, if impacting particles are completely molten, a microcrystalline, metastable, oxygen deficient phase is formed which has a simple cubic structure with lattice parameter of about 0.3 nm [12]. Although oxygen is rapidly absorbed during heat treatment in air or oxygen between 300 and 600°C , heat treatment at temperatures of $800\text{--}950^\circ\text{C}$ is necessary to form a superconductive deposit with critical temperature of $86\text{--}90$ K. There are indications that heat treatment of sintered $\text{YBa}_2\text{Cu}_3\text{O}_x$ at $400\text{--}500^\circ\text{C}$ in oxygen is necessary to develop the optimum structure in which $x = 7$ [15]. A few papers have reported the effect of annealing on the structure and properties of thermally sprayed coatings [3, 4, 8].

Copper is lost during the thermal spraying process and the original powder must contain additional Cu if a deposit with Y:Ba:Cu ratio of 1:2:3 is to be achieved [6]. Although many papers have reported critical temperatures of around 90 K with a sharp superconducting transition, the reported transport critical current densities (J_c) have been disappointingly low, often less than 100 A cm^{-2} . Clearly, much higher values of J_c must be achieved if technical products are to be made by the thermal spraying technique.

The critical current density is related to microstructure, as well as to the crystal structure of individual grains in polycrystalline aggregates, so that microstructural development of coatings during heat treatment is of considerable importance. A J_c of $\approx 130\text{ A cm}^{-2}$ has been achieved in this laboratory, for a flame-sprayed coating containing Cu in excess of the 1:2:3 ratio, after heat treatment at 950°C . The superior performance of this material was attributed to the development of a large grain size, due to the presence of a liquid phase at the annealing temperature [16].

The highest J_c reported so far for thermally sprayed coating (690 A cm^{-2}) was achieved by low-pressure plasma spraying on to a substrate heated to 650°C . The as-sprayed structure was reported to be "crystallographically disordered" and subsequent heat treatment for 1 h at 950°C in oxygen was required to achieve a high critical current density [11].

The present paper reports a systematic study of the microstructure of air plasma-sprayed material as a function of heat treatment at 950°C in air followed by annealing in flowing oxygen at $400\text{--}500^\circ\text{C}$.

2. Experimental procedure

Powder was produced by mixing, in the stoichiometric atomic ratio Y:Ba:Cu = 1:2:4, the following compounds: CuO (purity 98%) Y_2O_3 (purity 99.9%) Ba $(\text{NO}_3)_2$ (purity 99.5%). After being dry mixed the powder was calcined at 930°C for 24 h, then crushed and sieved to particle size range -56 to $+28\ \mu\text{m}$. This procedure was repeated several times until the quantity of powder was sufficient to spray.

The arc plasma spraying process was carried out using a SG-100 gun of Plasmadyne (Miller Thermal Technologies Inc., Tustin, CA) installed on an industrial robot. The torch was reconstructed to enable external injection of powder. The plasma spray parameters are listed in Table I. The coatings were deposited on to grit blasted mild steel up to the thickness of

TABLE I Plasma spray parameters

Primary gas: argon (SLPM)	30
Secondary gas: helium (SLPM)	15
Carrier gas: argon (SLPM)	4.5
Current (A)	950
Voltage (V)	44
Spray distance (mm)	100
Powder feed rate (g min ⁻¹)	15–22
Traverse speed (mm min ⁻¹)	700
Number of passes	15
Compressed air cooling	Yes
Compressed air thermal barrier	Yes

700–1000 μm . For further investigations the coatings were detached from the substrate and free-standing material was submitted to successive heat treatments. High-temperature heat treatment was carried out in a muffle furnace (Selby Co., Sydney, Australia) in air at 950 °C for the times of 3, 20 and 100 h. The material was subsequently annealed in a tube furnace (Lindberg, Watertown, WI) in flowing oxygen at temperatures of 400–500 °C for times varying from 24–36 h.

Particle sizes of the powder used to spray were determined with a particle size analyser Sedigraph 5100 (Micromeritics, Norcross, GA). The microstructure of sprayed coatings were examined by scanning electron microscopy (SEM) (Jeol JSM 840A) and optical microscopy (Reichert, Vienna). The specimens for optical microscopy have been prepared with the use of a grinding and polishing machine Planopol-Pedemax (Struers, Copenhagen) following the procedure described in [17]. Differential thermal analysis (DTA) investigations were made using Rigaku equipment at a heating rate of 20 K min⁻¹. X-ray diffraction (XRD) was carried out with a Scintag X-ray set-up equipped with PAD-5 goniometer using CuK α radiation.

Chemical analyses of powders and sprayed deposits were carried out by Atomic Absorption Spectroscopy using ICP on three independent samples. The bulk density, porosity and medium pore diameter of coatings were determined by mercury intrusion porosimetry (Micromeritics).

3. Results

3.1. Powder

The powder used for spraying had a median diameter of 36 μm . The chemical composition of the powder (Table II) corresponded to a Y:Ba:Cu ratio of approximately 1:2:4. X-ray diffraction of the powder showed the presence of the orthorhombic 1-2-3 phase (unit cell parameters $a = 0.382$ nm, $b = 0.3884$ nm,

$c = 1.1677$ nm) and CuO, as expected (Fig. 5a). Optical microscopy of a sample of powder embedded in epoxy resin and polished (Fig. 1) showed that the individual particles were not homogeneous, but contained various proportions of a bright phase, which was attributed from XRD, to copper oxide.

3.2. As-sprayed material

The chemical composition of the deposit (Table II) corresponds to Y:Ba:Cu = 1:2.0:3.0. XRD of the as-sprayed material (Fig. 2) showed broad peaks which can be attributed to the simple cubic structure with cell dimension $a = 0.2982$ nm (Table III). The phase was previously reported in flame-sprayed coatings [12]. The second detected phase in as-sprayed material was Y₂O₃ (ASTM card no. 25-1200). Y₂O₃ has also been observed previously in as sprayed coatings by Neiser *et al.* [6].

The coating contained many cracks (Fig. 3), arising from residual stresses generated during the spraying process, resulting in an open porosity of 4.8% (Table IV). Because the powder initially had the composition of 1:2.1:4.1, loss of Cu and Ba during spraying is evident.

The DTA curves for an as-sprayed coating and coatings which had been subsequently heat treated at 950 °C for 3 and 100 h are shown in Fig. 4. The as-sprayed coating exhibited endotherms at ≈ 800 , 905 and 1000 °C. After 3 h at 950 °C the peak at ≈ 800 °C persisted, but with reduced area, that at ≈ 905 °C was considerably reduced in size and a new endotherm appeared at 930 °C. After 115 h at 950 °C,

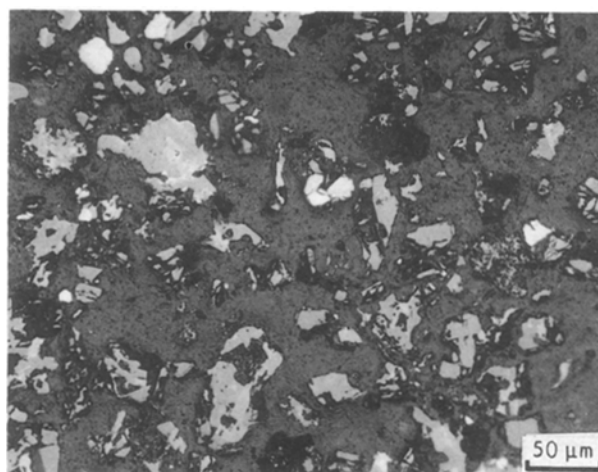


Figure 1 Optical microphotograph of particles of the powder used for spraying. The white grains correspond to CuO.

TABLE II Chemical composition of powder used to spray and as-sprayed coating

	Ba content (wt %)		Y content (wt %)		Cu content (wt %)	
	Mean value	S.D.	Mean value	S.D.	Mean value	S.D.
Powder	36.83	0.64	11.57	0.45	34.13	0.25
As-sprayed coating	41.10	0.36	13.58	1.00	28.97	0.51

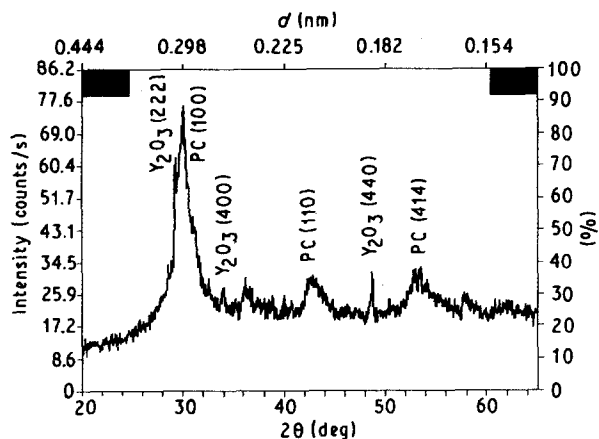


Figure 2 XRD of as-sprayed material.

TABLE III Diffraction pattern of simple cubic phase with cell constant $a = 0.2982$ nm

(hkl)	2θ (deg)	d(nm)
100	29.9412	0.2982
110	42.8551	0.2108
111	53.1578	0.1722
200	62.2152	0.1491
210	70.5679	0.1334
211	78.5082	0.1217
220	93.8817	0.1054



Figure 3 Cross-section of as-sprayed coating.

the 905 °C endotherm was very small, that at 800 °C disappeared and the endotherm at 930 °C persisted.

3.3. Heat-treated material

A heat-treatment temperature of 950 °C was chosen arbitrarily, as indicated from previous experience with

TABLE IV Bulk density open porosity and median pore diameter in the coatings as-sprayed and heat-treated at 950 °C in air for different periods of time

Time of heat treatment (h)	Bulk density (g cm^{-3})	Open porosity (%)	Median pore diameter (μm)
As-sprayed sample	5.13	4.8	57.9
3	5.36	2.9	1.1
95 ^a	–	2.6	0.4

^a Also annealed in flowing oxygen at 500 °C for 24 h.

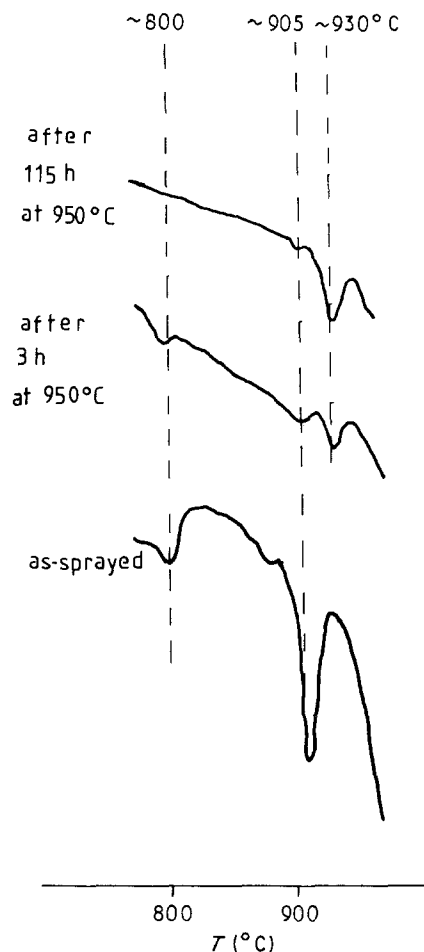


Figure 4 DTA of as-sprayed material and after heat treatment at 950 °C in air for 3 and 120 h. Heating rate was 20 °C min⁻¹.

flame-sprayed material [12, 13, 16]. XRD of a specimen heat treated for 3 h showed that it has transformed from the simple cubic phase to $\text{YBa}_2\text{Cu}_3\text{O}_x$ but with significant proportions of BaCuO_2 and Y_2BaCuO_5 present. Heat treatment for 20 h showed only peaks for the 1:2:3 phase (Fig. 5).

The XRD pattern of $\text{YBa}_2\text{Cu}_3\text{O}_x$ around $2\theta = 47^\circ$ shows three peaks corresponding to the 006, 020 and 200 planar spacings of the orthorhombic phase, and the 006, 200 spacings of the tetragonal phase [18]. These peaks provide a convenient indicator of the crystal structure because the a , b and c parameters depend upon oxygen content [18, 19]. In the case of material heat treated for 3 h, only a very broad hump was observed, but after 20 and 100 h the 006, 020

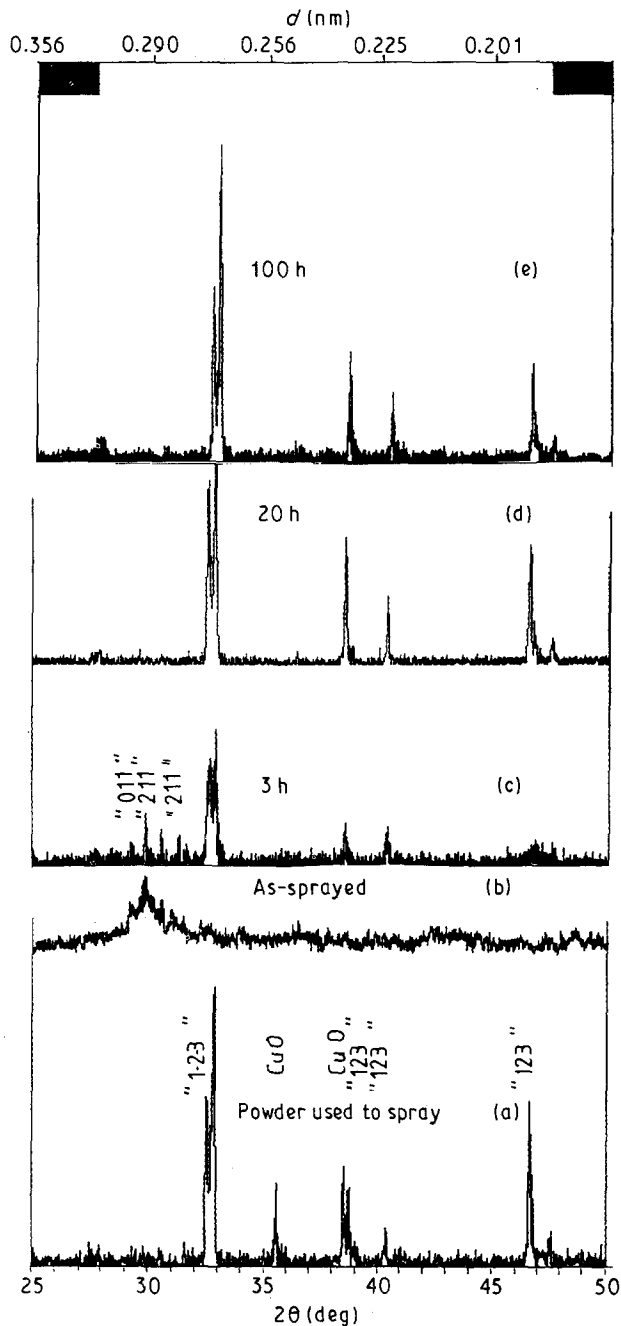


Figure 5 X-ray diffraction patterns of (a) $\text{YBa}_2\text{Cu}_3\text{O}_x$ powder used to spray, (b) as-sprayed material, and as-sprayed materials heat treated at 950°C in air for (c) 3 h, (d) 20 h and (e) 100 h.

peaks and 200 peak typical of the orthorhombic phase quenched from $400\text{--}500^\circ\text{C}$, that is $x \approx 6.9$, were observed, together with an additional peak corresponding to a lattice parameter of 0.194 nm (Fig. 6). Further heat treatment at 500 and 400°C in oxygen gave a reduction in the intensity of this additional peak and a small shift in lattice parameter.

SEM of the surface of the heat-treated samples showed that the surface morphology of the material heat treated for 3 h at 950°C was similar to the as-sprayed coating but, after 20 h, crystals of tens of micrometres diameter were observed and after 100 h elongated grains up to $100\ \mu\text{m}$ in size were formed. SEM of a fracture surface shows the large planar grains produced by heat treatment for 100 h at 950°C , and in many cases, the grains appear not to be in contact (Fig. 7). Optical microscopy showed large

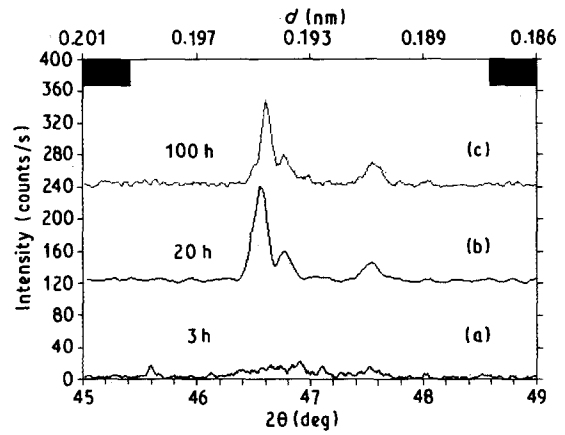


Figure 6 Region of X-ray diffraction patterns from $2\theta = 46^\circ$ to $2\theta = 48^\circ$ corresponding to material heat treated at 950°C in air for (a) 3 h, (b) 20 h and (c) 100 h.

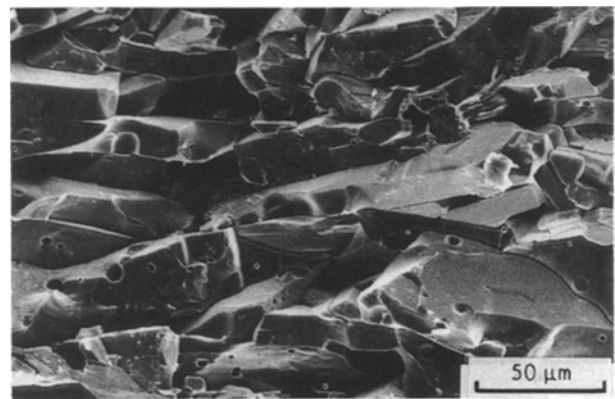


Figure 7 SEM of fractured surface of the material heat-treated at 950°C in air for 3 and 100 h followed by annealing in flowing oxygen at 500°C for 24 h.

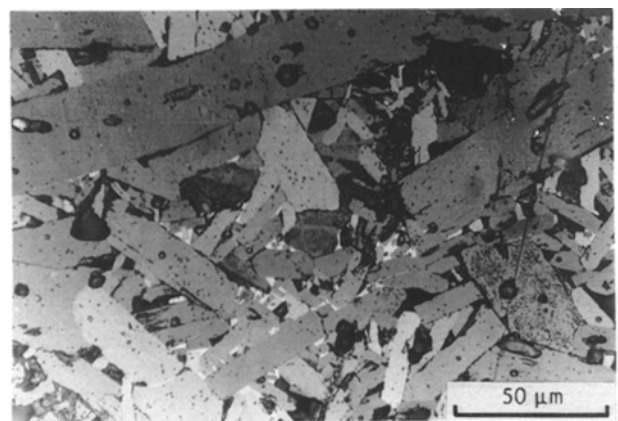


Figure 8 Cross-section of the sample heat-treated at 950°C in air for 20 h and annealed at 400°C in flowing oxygen for 48 h. White grains probably correspond to CuO .

finely twinned crystals in the material heat treated for 100 h at 950°C in more detail (Fig. 8) with evidence of bright regions at some grain boundaries which may be CuO .

4. Discussion

The powder used for spraying was deliberately prepared with excess Cu , to allow for the reported loss of

Cu during spraying, to give a coating with composition close to Y:Ba:Cu = 1:2:3. Although X-ray diffraction showed that the original powder contained only the phases $\text{YBa}_2\text{Cu}_3\text{O}_x$ and CuO, as expected from its composition, optical microscopy of polished sections of the particles clearly showed a considerable variation of CuO content from particle to particle. Because particles take different trajectories in the plasma jet during spraying and are thus subject to different thermal histories, the copper loss would be expected to vary from particle to particle. Therefore, the range of compositions of individual lamellae within the coating would be expected to vary in the manner illustrated in Fig. 9.

The structure of the as-sprayed coating consisted predominately of the metastable, simple cubic phase previously reported in flame-sprayed coatings [12, 16] but with a small proportion of Y_2O_3 . The absence of residual $\text{YBa}_2\text{Cu}_3\text{O}_x$ in the deposit indicates that the powder injection arrangement and torch operating conditions used resulted in complete melting of the powder, a result not achieved in many other reports of the structure of plasma-sprayed $\text{YBa}_2\text{Cu}_3\text{O}_x$. This result, furthermore, suggests that the simple cubic structure is formed by rapid solidification of liquid with a range of compositions around the 1:2:3 proportions. The presence of a small amount of Y_2O_3 in the coating maybe explained by consideration of the Y_2O_3 , BaO, CuO phase diagram which shows a steeply rising liquidus surface, with Y_2O_3 as the primary crystalline phase, towards the Y_2O_3 corner of the system [20]. Thus the equilibrium structure of droplets which did not reach the liquidus temperature during the melting step of the spraying process would be liquid phase and crystals of Y_2O_3 . Small crystals of Y_2O_3 have, in fact, been observed by transmission electron microscopy of as-sprayed coatings [6]. Samples of $\text{YBa}_2\text{Cu}_3\text{O}_x$, rapidly quenched from 1500 °C have been shown to contain large crystals of Y_2O_3 [21].

Heat treatment of the as-sprayed deposit at 950 °C for 3 h resulted in the formation of $\text{YBa}_2\text{Cu}_3\text{O}_x$, plus

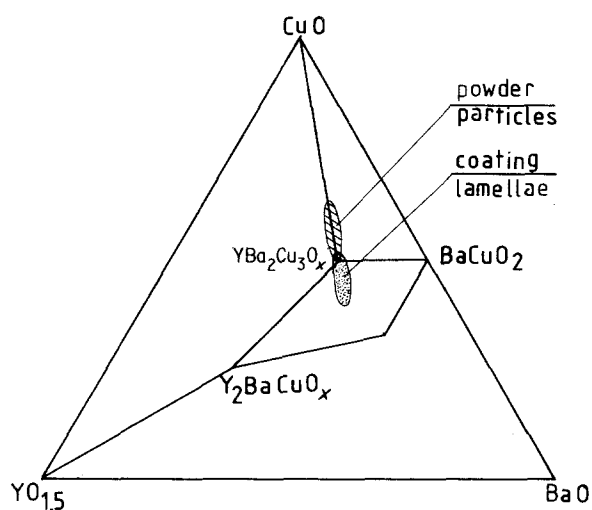


Figure 9 Phase diagram showing estimated composition range of powder and coating.

some BaCuO_2 and Y_2BaCuO_5 . This is consistent with a range of compositions of the lamellae as shown in Fig. 9 although the average composition of the coating, from chemical analysis, was close to the 1:2:3 proportions. Heat treatment for periods of time greater than 20 h at 950 °C, however, resulted in XRD patterns corresponding to the single-phase $\text{YBa}_2\text{Cu}_3\text{O}_x$ indicating that the compositional variations within the as-sprayed deposit had levelled out by diffusion.

The XRD patterns observed for samples heat treated at 950 °C for more than 20 h, and slowly cooled in air, in particular the group of peaks near $2\theta = 47^\circ$, show that the material consists predominately of orthorhombic $\text{YBa}_2\text{Cu}_3\text{O}_x$ with lattice parameters consistent with $x \approx 6.9$; however, there is evidence that some orthorhombic phase is also present with a lower oxygen content. Further heat treatment in oxygen at 400–500 °C resulted in complete oxidation to give a homogeneous material.

The Y_2O_3 , BaO, CuO phase diagram [20] shows that the equilibrium structure at 950 °C would be $\text{YBa}_2\text{Cu}_3\text{O}_x$ plus a liquid phase for compositions containing excess CuO. A large DTA endotherm showed that liquid phase was formed at about 900 °C on heating the as-sprayed coating, which corresponds to the phase equilibrium $\text{YBa}_2\text{Cu}_3\text{O}_x + \text{BaCuO}_2 + \text{CuO} \rightarrow \text{L}$ [20] but the decrease in the endotherm area and appearance of a 930 °C endotherm after extended heat treatment at 950 °C shows that the liquid phase composition moves towards the equilibrium $\text{BaCuO}_2 + \text{CuO} \rightarrow \text{L}$ and/or $\text{YBa}_2\text{Cu}_3\text{O}_x + \text{CuO} \rightarrow \text{Y}_2\text{BaCuO}_5 + \text{L}$ [20]. The range of compositions postulated in as-sprayed material (Fig. 9) would explain the formation of a significant proportion of liquid at 950 °C even though the average composition was close to 1:2:3. (Pure $\text{YBa}_2\text{Cu}_3\text{O}_x$ melts incongruently at 1010 °C [20].) The presence of this liquid would be expected to favour grain growth and interdiffusion to give the large crystals of uniform composition observed in the microstructure but the proportion of liquid phase would decrease as the structure homogenized to $\text{YBa}_2\text{Cu}_3\text{O}_x$. This is supported by the small endotherm at $\approx 930^\circ\text{C}$ observed in heat-treated material. The formation of gaps between the grains of the coating heat treated at 950 °C for 100 h (Fig. 7) has probably arisen from the gradual reduction in volume of a transient liquid phase at grain boundaries as the composition moved towards homogeneous $\text{YBa}_2\text{Cu}_3\text{O}_x$.

At 950 °C the 1:2:3 phase would have the tetragonal structure with low oxygen content. Although slow cooling in air is apparently sufficient to restore the oxygen content to give $x \approx 6.9$, a residual of lower oxygen phase is present which can be eliminated by further heat treatment in oxygen at 400–500 °C.

The plasma spraying process is capable of producing a coating of predominately $\text{YBa}_2\text{Cu}_3\text{O}_7$ after prolonged heat treatment at 950 °C in air. It is now generally agreed that the critical current density of superconducting polycrystalline $\text{YBa}_2\text{Cu}_3\text{O}_7$ is limited because of "weak links" between the grains which may arise from inherent grain-boundary effects [22],

grain-boundary phases [23] and grain-boundary pores.

The strong influence of grain-boundary structure on critical current density of polycrystalline $\text{YBa}_2\text{Cu}_3\text{O}_7$ is a major factor inhibiting the achievement of high critical current density and further work is required to control the microstructure of plasma-sprayed coatings to achieve acceptable properties. A major limitation of the microstructures reported in the present study is the limited contact at grain boundaries, after extended heat treatment at 950°C , which probably is a result of the absorption of a transient liquid phase.

5. Conclusions

1. Plasma spraying of $\text{YBa}_2\text{Cu}_3\text{O}_x$ results in considerable loss of Cu and powder with Y:Ba:Cu ratio of around 1:2:4 is necessary to form a coating with the 1:2:3 composition.

2. The as-sprayed material consists of a fine-grained metastable simple cubic structure with lattice parameter $a = 0.2982\text{ nm}$.

3. Heat treatment of as-sprayed material at 950°C in air results in the formation of a transient liquid phase which leads to the formation of a large grain size, polycrystalline orthorhombic $\text{YBa}_2\text{Cu}_3\text{O}_x$ microstructures on slow cooling. Heat treatment for at least 20 h is required to eliminate inhomogeneities in composition introduced from the inhomogeneous powder and variations of Cu concentrations produced during spraying.

4. Further heat treatment at $400\text{--}500^\circ\text{C}$ in oxygen results in a more uniform degree of oxidation of the grains.

Acknowledgements

This project has been supported by Generic Technology Grant Agreement no. 15011. Dr Mary Gani is thanked for discussions concerning DTA technique and Mr Rod Mackie for providing XRD patterns.

References

1. M. K. WU, J. R. ASHBURN, C. J. TORNG, P. H. HOR, R. L. MENG, L. GAO, Z. J. HUANG, Y. Q. WANG and C. W. CHU, *Phys. Rev. Lett.* **58** (1987) 908.

2. J. P. KIRKLAND, R. A. NEISER, H. HERMAN, W. T. ELAM, S. SAMPATH, E. F. SKELTON, D. GANSERT and H. G. WANG, *Adv. Ceram. Mater.* **2** (3B) (1987) 401.
3. J. J. CUOMO, C. R. GUARNIERI, S. A. SHIVASHANKAR, R. A. ROY, D. S. YEE and R. ROSENBERG, *ibid.* **2** (3B) (1987) 422.
4. W. F. CHU and F. T. ROHR, *Phys. Chem.* **153-155** (1988) 802.
5. L. S. WEN, S. W. QIAN, Q. Y. HU, K. GUAN and Y. Z. ZHUANG, *Thin Solid Films* **168** (1989) 231.
6. R. A. NEISER, Y. M. ZHU, H. HERMAN and B. GÜDMUNDSSON, in "Proceedings of the 12th International Thermal Spraying Conference", London, 4-9 June, 1989, edited by I. A. Bucklow (Welding Institute, Abington, UK, 1989) Vol. 2, p. 205.
7. C. M. LIAO, X. L. CHEN, X.-W. QI and D.-M. DU, *ibid.*, Paper 20, Vol. 2, p. 227.
8. S. KITAHARA, Y. YOSHIDA, T. FUKUSHIMA, S. KURODA, K. INOUE, H. MAEDA and M. FUNAHI, *ibid.*, Paper 86, Vol. 2, p. 237.
9. J. LU and G. W. QIAO, *Mod. Phys. Lett. B.* **2** (1988) 661.
10. T. ASANO, K. TRAN, A. S. BYRNE, M. M. RAHMAN, C. Y. YAND and J. D. REARDON, *Appl. Phys. Lett.* **54** (1989) 1275.
11. T. TACHIKAWA, I. WATANABE, S. KOSUGE, M. KABASAWA, T. SURUKI, Y. MOTSUDA and Y. SHINBO, *ibid.* **52** (1988) 1011.
12. G. N. HEINTZE and R. McPHERSON, *Mater. Sci. Forum* **34-36** (1988) 345.
13. G. HEINTZE, R. McPHERSON, D. TOLINO and C. ANDRIKIDIS, *J. Mater. Sci. Lett.* **7** (1988) 251.
14. P. MCGINN, N. TAIN, V. ANAND and D. LEE, *Thin Solid Films* **166** (1988) 163.
15. H. M. O'BRYAN and P. K. GALLAGHER, *Adv. Ceram. Mater.* **2** (3B) (1987) 640.
16. R. McPHERSON, G. N. HEINTZE, D. TOLINO and E. DE JONG, in "Proceedings of the 12th International Thermal Spraying Conference", London, 4-9 June edited by I. A. Bucklow (Welding Institute, Abington, UK, 1989) Vol. 2, p. 249.
17. M. LEMCKE and B. ADLER, *Structure, Struers Metallogr. News* **18**(1) (1989) 3.
18. P. K. GALLAGHER, H. M. O'BRYAN, S. A. SUNSHINE and D. W. MURPHY, *Mater. Res. Bull.* **22** (1987) 995.
19. H. M. O'BRYAN and P. K. GALLAGHER, *J. Mater. Res.* **3** (1988) 619.
20. T. ASELAGI and K. KEEFER, *ibid.* **3** (1988) 1279.
21. M. MURAKAMI, M. MORITA, K. DOI, K. MIYAMOTO and H. HAMADA, *Jpn. J. Appl. Phys.* **28** (1989) 399.
22. D. DIMOS, P. CHAUDHARI, J. MANNHART and F. K. LE GOVES, *Phys. Rev. Lett.* **61** (1988) 219.
23. R. A. CAMPO, J. W. EVENTS, B. A. GLOWACKI, S. B. NEWCOMB, R. A. SOMEKH and W. M. STOBBS, *Nature* **329** (1987) 229.

Received 13 March
and accepted 6 November 1990